

Exclusive generation of rat spermatozoa in sterile mice utilizing blastocyst complementation with pluripotent stem cells

Joel Zvick,¹ Monika Tarnowska-Sengül,¹ Adhideb Ghosh,^{1,4} Nicola Bundschuh,¹ Pjeter Gjonlleshaj,¹ Laura C. Hinte,² Christine L. Trautmann,¹ Falko Noé,^{1,4} Xhem Qabrati,¹ Seraina A. Domenig,¹ Inseon Kim,¹ Thomas Hennek,³ Ferdinand von Meyenn,² and Ori Bar-Nur^{1,*}

¹Laboratory of Regenerative and Movement Biology, Department of Health Sciences and Technology, ETH Zurich, Schwerzenbach 8603, Switzerland

²Laboratory of Nutrition and Metabolic Epigenetics, Department of Health Sciences and Technology, ETH Zurich, Schwerzenbach 8603, Switzerland

³ETH Phenomics Center, ETH Zurich, Zurich 8049, Switzerland

⁴Functional Genomics Center Zurich, ETH Zurich and University of Zurich, Zurich 8057, Switzerland

*Correspondence: ori.bar-nur@hest.ethz.ch

<https://doi.org/10.1016/j.stemcr.2022.07.005>

SUMMARY

Blastocyst complementation denotes a technique that aims to generate organs, tissues, or cell types in animal chimeras via injection of pluripotent stem cells (PSCs) into genetically compromised blastocyst-stage embryos. Here, we report on successful complementation of the male germline in adult chimeras following injection of mouse or rat PSCs into mouse blastocysts carrying a mutation in *Tsc22d3*, an essential gene for spermatozoa production. Injection of mouse PSCs into *Tsc22d3*-Knockout (KO) blastocysts gave rise to intraspecies chimeras exclusively embodying PSC-derived functional spermatozoa. In addition, injection of rat embryonic stem cells (rESCs) into *Tsc22d3*-KO embryos produced interspecies mouse-rat chimeras solely harboring rat spermatids and spermatozoa capable of fertilizing oocytes. Furthermore, using single-cell RNA sequencing, we deconstructed rat spermatogenesis occurring in a mouse-rat chimera testis. Collectively, this study details a method for exclusive xenogeneic germ cell production *in vivo*, with implications that may extend to rat transgenesis, or endangered animal species conservation efforts.

INTRODUCTION

Pluripotent stem cells in the form of ESCs or induced pluripotent stem cells (iPSCs) hold a unique propensity to differentiate into any cell type of the adult organism, including germ cells (Saitou and Miyauchi, 2016). Furthermore, injection of mouse or rat PSCs into blastocysts can produce adult chimeras that harbor PSC contribution to all cell types and organs including the germline, thus rendering genetically modified PSCs a commonly used method for the production of transgenic animals (Wu et al., 2016). However, the quality of ESCs or iPSCs is often-times impaired due to genetic or epigenetic aberrations, precipitating reduced contribution to chimerism and to the germline. These undesirable attributes may complicate production of transgenic animal models that are reliant on germline transmission to establish animal colonies, warranting methods that augment PSC contribution to the germline highly valuable.

Blastocyst complementation is an innovative technology that enables production of specific cell types or organs in chimeras via injection of PSCs into blastocysts carrying organ or cell type-disabling genetic mutations, thereby unfolding a developmental niche receptive for exclusive generation of specific cell types or organs from injected PSCs (Wu et al., 2016). A seminal study performed in the 1990s was the first to demonstrate injection of mouse ESCs (mESCs) into recombination-activating gene-2 (RAG-2) mutated mouse blastocysts (Chen et al., 1993a,

1993b). As RAG-2-deficient mice cannot produce mature lymphocytes, intraspecies chimeras harbored B and T cells that were solely derived from the injected ESCs (Chen et al., 1993a, 1993b). Follow-up studies have recently reported on production of PSC-derived kidney, lung, bone, forebrain, and vascular endothelium using blastocyst complementation in mice (Chang et al., 2018; Chubb et al., 2017; Hamanaka et al., 2018; Kitahara et al., 2020; Mori et al., 2019; Usui et al., 2012). Similarly, recent studies have reported successes in using intraspecies blastocyst complementation to produce tissues and organs in pigs (Matsunari et al., 2013, 2020; Zhang et al., 2018).

Animal chimeras carrying two distinct genotypes were first reported for two murine species, *Mus musculus* and *Mus caroli* (Rossant and Frels, 1980). Further, blastocyst complementation between mice and rats has been documented in groundbreaking studies that reported on xenogeneic pancreas formation in interspecies chimeras following injection of PSCs into *Pdx1*-KO blastocysts (Kobayashi et al., 2010; Wu et al., 2017; Yamaguchi et al., 2017). Additional studies have harnessed interspecies blastocyst complementation to exclusively generate blood vasculature, kidneys, or thymi in mice or rats (Goto et al., 2019; Isotani et al., 2011; Wang et al., 2020).

Blastocyst complementation may further provide an attractive approach to generate germ cells solely from injected PSCs (Wu et al., 2016). Notably, such method may aid in production of transgenic animals using PSCs that do not contribute well to the germline, as a vacant germline

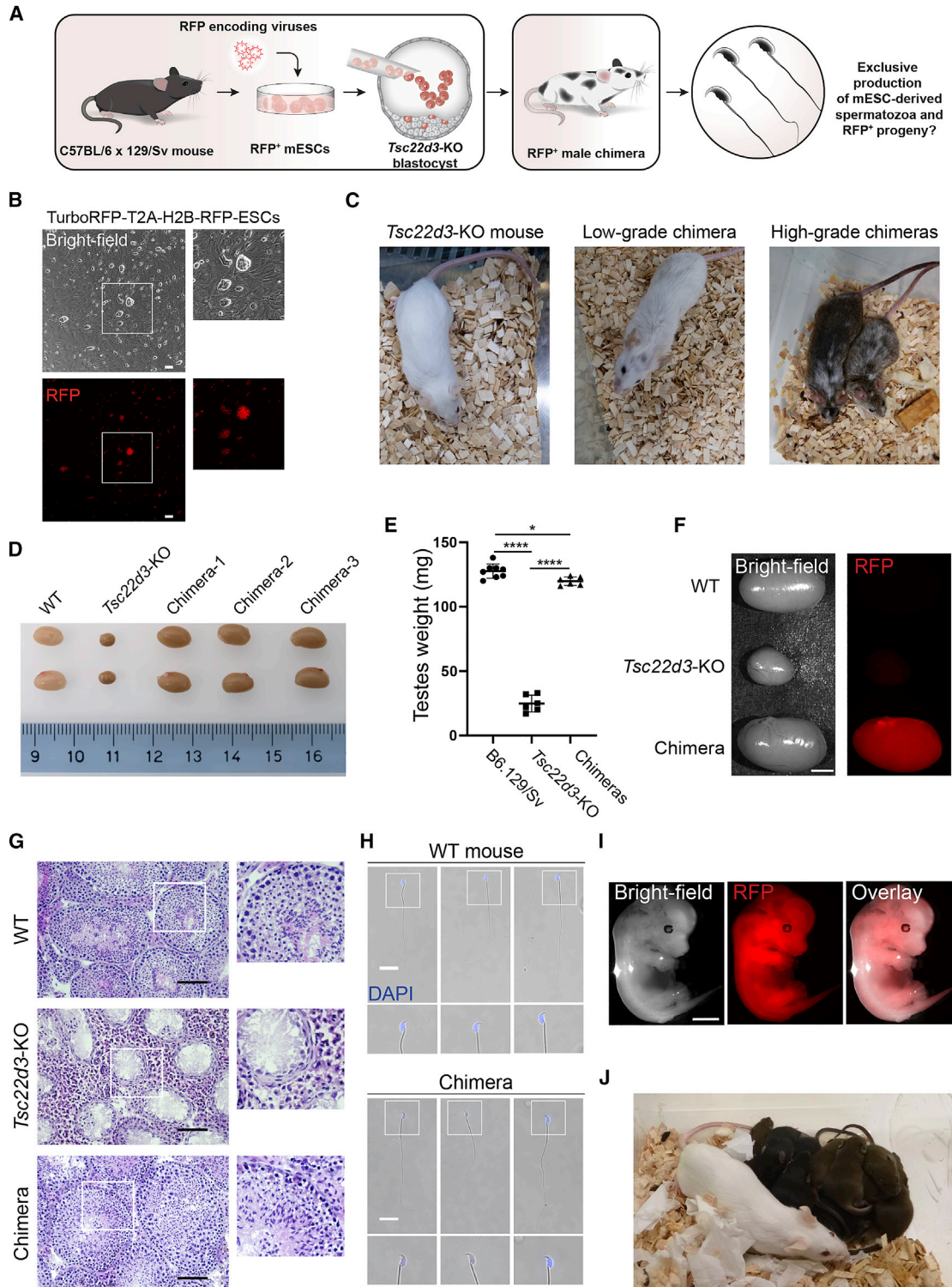


Figure 1. Exclusive generation of mESC-derived spermatozoa in intraspecies chimeras

(A) A schematic illustrating experimental design. mESCs, mouse embryonic stem cells. RFP, red fluorescent protein, KO, knockout.

(B) Representative bright-field and RFP images of KH2-mESCs transduced with lentiviruses encoding for constitutive *EF1 α -TurboRFP-T2A-H2B-RFP* reporter expression. Scale bar, 100 μ m.

(legend continued on next page)



niche may reduce competition with host germ cells and enable increased formation of gametes from the injected PSCs (Koentgen et al., 2016; Miura et al., 2021; Taft et al., 2013). In addition, intraspecies blastocyst complementation in mice may reduce the necessity to breed large numbers of chimeras to achieve germline transmission, thereby reducing animal husbandry costs and mitigating animal burden (Koentgen et al., 2016; Taft et al., 2013). This method may also prove useful for interspecies blastocyst complementation in rats, which provide an excellent biomedical research model for a plethora of human conditions. Rat PSCs oftentimes do not contribute well to the germline, and transgenic techniques such as blastocyst injection and embryo transfer are not as widely established as with mice. As such, germline blastocyst complementation using genetically modified rat PSCs in sterile mice may enable exclusive production of transgenic rat gametes, thus assisting in the production of rat models for biomedical research.

Spermatogenesis is a complex biological process that manifests via spermatogonial stem cell differentiation into mature haploid spermatozoa in a unidirectional stepwise trajectory. Genetic mutations in genes that are critical for this differentiation process can lead to sterility and complete lack of mature spermatozoa in adult animals (Saitou and Yamaji, 2010). For example, mutations in the X-linked glucocorticoid-induced leucine zipper gene (*Gilz*, also known as *Tsc22d3*), have been well-established to inflict sterility in male mice (Bruscoli et al., 2012; Koentgen et al., 2016; Ngo et al., 2013; Romero et al., 2012; Suarez et al., 2012). Absence of the TSC22D3 protein manifests in azoospermia and male infertility as a consequence of arrest in spermatogenesis during meiosis I, resulting in extensive atrophy of the testes and absence of spermatozoa in adult *Tsc22d3*-KO mice (Bruscoli et al., 2012; Koentgen et al., 2016; Ngo et al., 2013; Romero et al., 2012; Suarez et al., 2012). As a result, *Tsc22d3*-KO mice have been recently used to preferentially produce functional mouse spermatozoa from injected ESCs (Koentgen et al., 2016). Building upon this finding, here we set out to explore whether injection of mouse iPSCs (miPSCs) or rESCs into *Tsc22d3*-KO blastocysts can overcome the sterility asso-

ciated with the *Tsc22d3* mutation in male intra- or interspecies chimeras and produce functional spermatozoa which are solely derived from the injected PSCs.

RESULTS

Injection of mESCs into *Tsc22d3*-KO blastocysts produces intraspecies chimeras exclusively carrying functional mouse spermatozoa

We commenced our investigation with injection of mESCs into *Tsc22d3*-KO blastocysts to assess whether injected cells can contribute to chimerism and generate functional mouse spermatozoa that are solely derived from injected ESCs as previously reported (Koentgen et al., 2016) (Figures 1A and S1A). The *Tsc22d3*-KO blastocysts were generated by crossing homozygous *Tsc22d3*-floxed females with homozygous *Rosa26-Cre* males (Koentgen et al., 2016). As the *Tsc22d3* gene is located on the X chromosome, this mating strategy ensures that all male progenies are hemizygous *Tsc22d3*-KO and sterile, whereas females are heterozygous and fertile (Figure S1A). As donor PSCs, we used KH2-mESCs, a subclone of V6.5 ESCs, and transduced cells with lentiviruses encoding for a constitutive cytoplasmic and nuclear red fluorescent protein (RFP) (Figure 1B) (Beard et al., 2006). Prior to injections of cells into *Tsc22d3*-KO blastocysts, we confirmed that RFP⁺KH2-mESCs maintained a normal diploid karyotype and expressed well-established pluripotency genes (Figures S1B and S1C). Following fluorescence-activated cell sorting (FACS)-purification for RFP⁺ cells and *in vitro* propagation, we injected 12 to 15 cells into *Tsc22d3*-KO blastocysts to produce RFP⁺KH2-mESC/*Tsc22d3*-KO chimeras, while concomitantly generating non-chimeric *Tsc22d3*-KO sterile male mice and fertile females (Figure 1C). Non-chimeric *Tsc22d3*-KO mice retained their albino fur color, whereas chimeric *Tsc22d3*-KO animals exhibited dark fur color emanating from the contribution of RFP⁺KH2-mESCs and demonstrating a diverse degree of coat color chimerism (Figure 1C). *Tsc22d3*-KO adult male mice were of normal

(C) Representative photos of a *Tsc22d3*-KO mouse (left), a low-grade RFP⁺KH2-ESCs/*Tsc22d3*-KO chimera (middle) and high-grade RFP⁺KH2-ESCs/*Tsc22d3*-KO chimeras (right).

(D) A representative photo of testes isolated from the indicated mouse strains.

(E) Quantification of testes weight for the indicated mouse strains ($n = 6-8$ biological replicates; each dot represents a single testicle, one-way ANOVA test with Tukey post hoc analysis was used, error bars denote SD, $*p < 0.05$, $***p < 0.0001$).

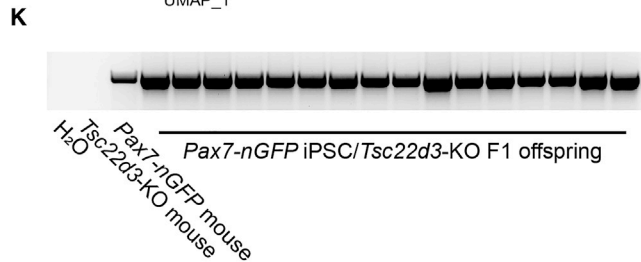
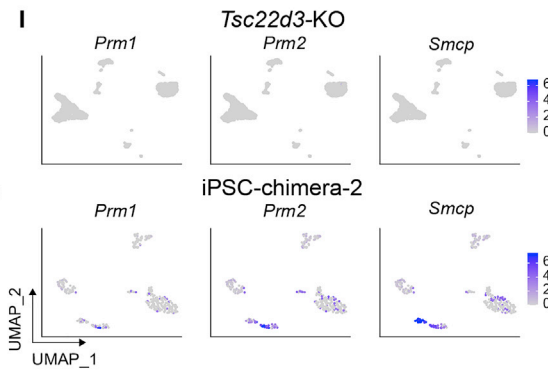
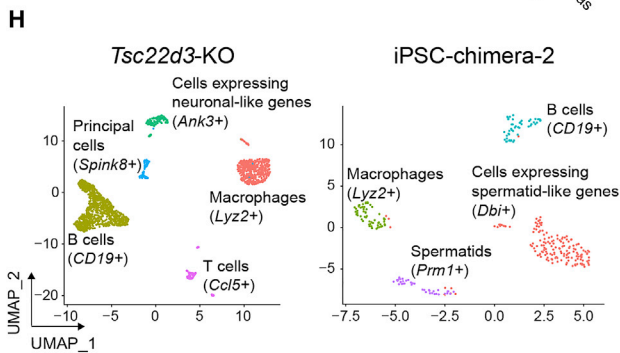
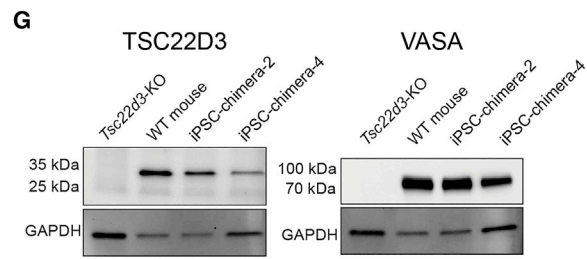
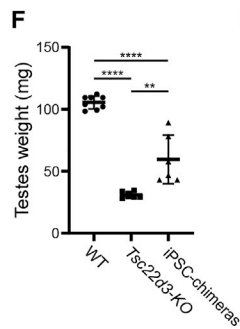
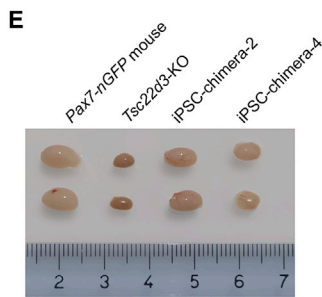
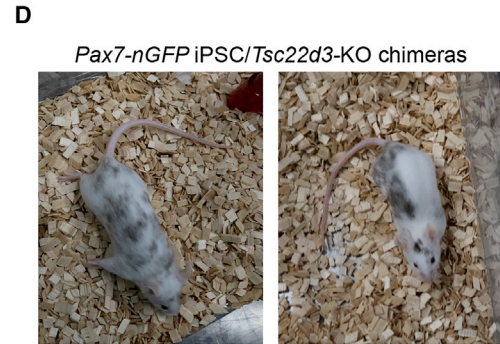
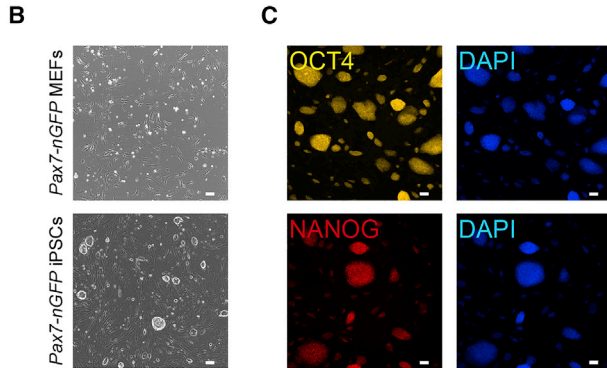
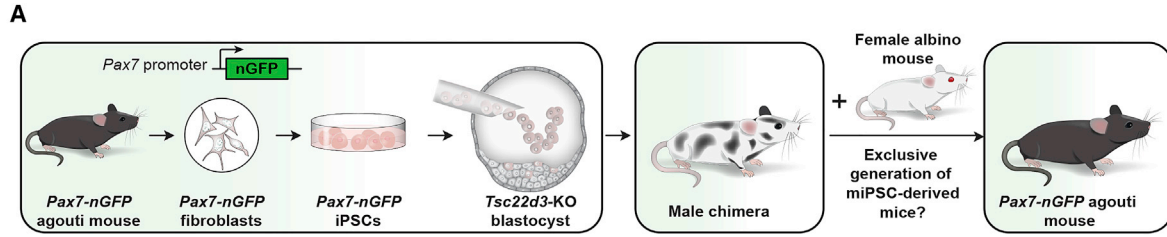
(F) Representative bright-field and RFP images of mouse testes isolated from the indicated strains. Scale bar, 2 mm.

(G) Testes cross-sections of the indicated samples stained with H&E. Scale bar, 100 μm .

(H) Representative images of spermatozoa extracted from the cauda epididymis of the indicated animals. Scale bar, 20 μm .

(I) Representative images of an E13.5 embryo generated from a cross between the F1 male progeny of an RFP⁺KH2-mESCs/*Tsc22d3*-KO chimera and a WT female mouse. Scale bar, 2 mm.

(J) A photo showing mouse pups derived via IVF with spermatozoa extracted from an RFP⁺KH2-mESCs/*Tsc22d3*-KO chimera and oocytes of an albino Swiss Webster mouse.



(legend on next page)



size and body weight; however, their testes were significantly smaller and weighed less in comparison with wild-type (WT) mice (Figures 1E and S1D). In contrast, chimeras' testes size and weight were slightly smaller than WT mouse testes of a similar genetic background, and most notably weighing 4 to 5 times more than testes harvested from *Tsc22d3*-KO mice (Figure 1E). Of note, complemented testes exhibited strong RFP expression, suggesting that lentiviral promoter silencing did not occur in several testicular cell types (Figure 1F). Cross-section of *Tsc22d3*-KO testes followed by staining with H&E demonstrated extensive seminiferous tubule atrophy and lack of spermatozoa (Figure 1G). In contrast, testes of RFP⁺KH2-mESC/*Tsc22d3*-KO chimeras exhibited WT-like seminiferous tubule structures containing spermatozoa, albeit due to transgene silencing RFP expression was not detected in VASA⁺ germ cells and was mostly confined to interstitial cells that expressed the Leydig cell marker HSD3B (Figures 1G, S1E–S1G). Notably, motile spermatozoa with intact tails and typical mouse sperm head-morphology were detected in the cauda epididymis of an RFP⁺KH2-mESC/*Tsc22d3*-KO chimera; however, were absent in the cauda of a *Tsc22d3*-KO mouse (Figure 1H and Video S1). Natural mating of chimeras' F1 offspring with WT mice produced RFP⁺ embryos, establishing the germline transmission potency of RFP⁺KH2-mESCs (Figure 1I). Last, *in vitro* fertilization (IVF) of oocytes from a Swiss Webster albino mouse strain with chimera spermatozoa only gave rise to progenies that had either a black or agouti fur coat color, emanating from the mixed C57BL/6 X 129/Sv genetic background of KH2-mESCs (Figure 1J). Based on these results, we confirmed that *Tsc22d3*-KO male mice embody a vacant developmental niche receptive for blastocyst complementation with mESCs as previously reported (Koentgen et al., 2016). As such, *Tsc22d3*-mutated embryos can be used to investigate blas-

tocyst complementation of the male germline with other PSC types.

Exclusive generation of miPSC-derived spermatozoa via blastocyst complementation

ESCs are rarely available from most animal species, rendering iPSCs a more accessible PSC source to produce intra- or interspecies germ cells via blastocyst complementation. Therefore, our next goal was to investigate whether injection of transgenic mouse iPSCs into *Tsc22d3*-KO embryos can exclusively produce iPSC-derived functional spermatozoa in chimeras that carry a transgenic allele (Figure 2A). To this end, we reprogrammed to pluripotency embryonic fibroblasts carrying a *Pax7-nuclear GFP* (*Pax7-nGFP*) reporter, which fluorescently labels skeletal muscle stem cells termed satellite cells, thus allowing for genotyping in F1 progeny (Sambasivan et al., 2009). Reprogramming of *Pax7-nGFP* mouse embryonic fibroblasts into iPSCs was performed using lentiviral vectors carrying a polycistronic doxycycline-inducible mouse *STEMCCA* cassette, an *M2rtTA* cassette, and medium containing ascorbic acid and GSK-3 β inhibitor, as previously described (Bar-Nur et al., 2014; Sommer et al., 2009). *Pax7-nGFP* iPSCs were dome-shaped, expressed pluripotency genes and maintained a normal diploid karyotype (Figures 2B, 2C, S2A, and S2B). Injection of *Pax7-nGFP* iPSCs into *Tsc22d3*-KO blastocysts gave rise to several chimeras as judged by dark coat color (Figure 2D and Table S2).

Testes weight and size of several *Pax7-nGFP* iPSC/*Tsc22d3*-KO chimeras were similar to those of *Tsc22d3*-KO mice; however, three chimeras showed increased testicular size and weight (Figures 2E, 2F, S2C, and Table S2). Of note, the more variable and lower testicular weight of miPSC-chimeras in comparison with mESC-chimeras may be attributed to enhanced contribution of KH2-mESCs to chimerism and

Figure 2. Exclusive production of miPSC-derived functional spermatozoa in chimeras

- (A) A schematic illustrating experimental design.
- (B) Representative bright-field images of *Pax7-nGFP* fibroblasts (top) and derivative *Pax7-nGFP* iPSCs (bottom). Scale bar, 100 μ m. MEFs, mouse embryonic fibroblasts.
- (C) Representative immunofluorescence images of OCT4 and NANOG in *Pax7-nGFP* iPSCs. Scale bar, 100 μ m.
- (D) Representative photos showing two adult male *Pax7-nGFP*-iPSC/*Tsc22d3*-KO chimeras. Agouti coat color indicates contribution of *Pax7-nGFP* iPSCs to chimerism.
- (E) A photo of testes isolated from the indicated mouse strains.
- (F) A graph depicting testes weight from the indicated mouse strains ($n = 4-8$ biological replicates; each dot represents a single testis, one-way ANOVA test with Tukey post hoc analysis was used, error bars denote SD, ** $p < 0.01$, **** $p < 0.0001$).
- (G) Western blot analysis for TSC22D3 and VASA protein expression in the indicated samples.
- (H) UMAP projections showing all cells colored by different cell types in PESA-derived cauda epididymis biopsies from the indicated animals. Note presence of "spermatids" only in the iPSC-chimera.
- (I) UMAP projections for the indicated elongated spermatid markers showing presence only in the iPSC-chimera cell populations shown in (H).
- (J) A photo showing the progeny of natural breeding between a *Pax7-nGFP*-iPSC/*Tsc22d3*-KO male chimera and an albino female mouse. Note that all F1 pups have an agouti coat color, indicating exclusive germline transmission from *Pax7-nGFP* iPSCs.
- (K) PCR analysis for the transgenic *Pax7-nGFP* allele in the indicated mouse strains.

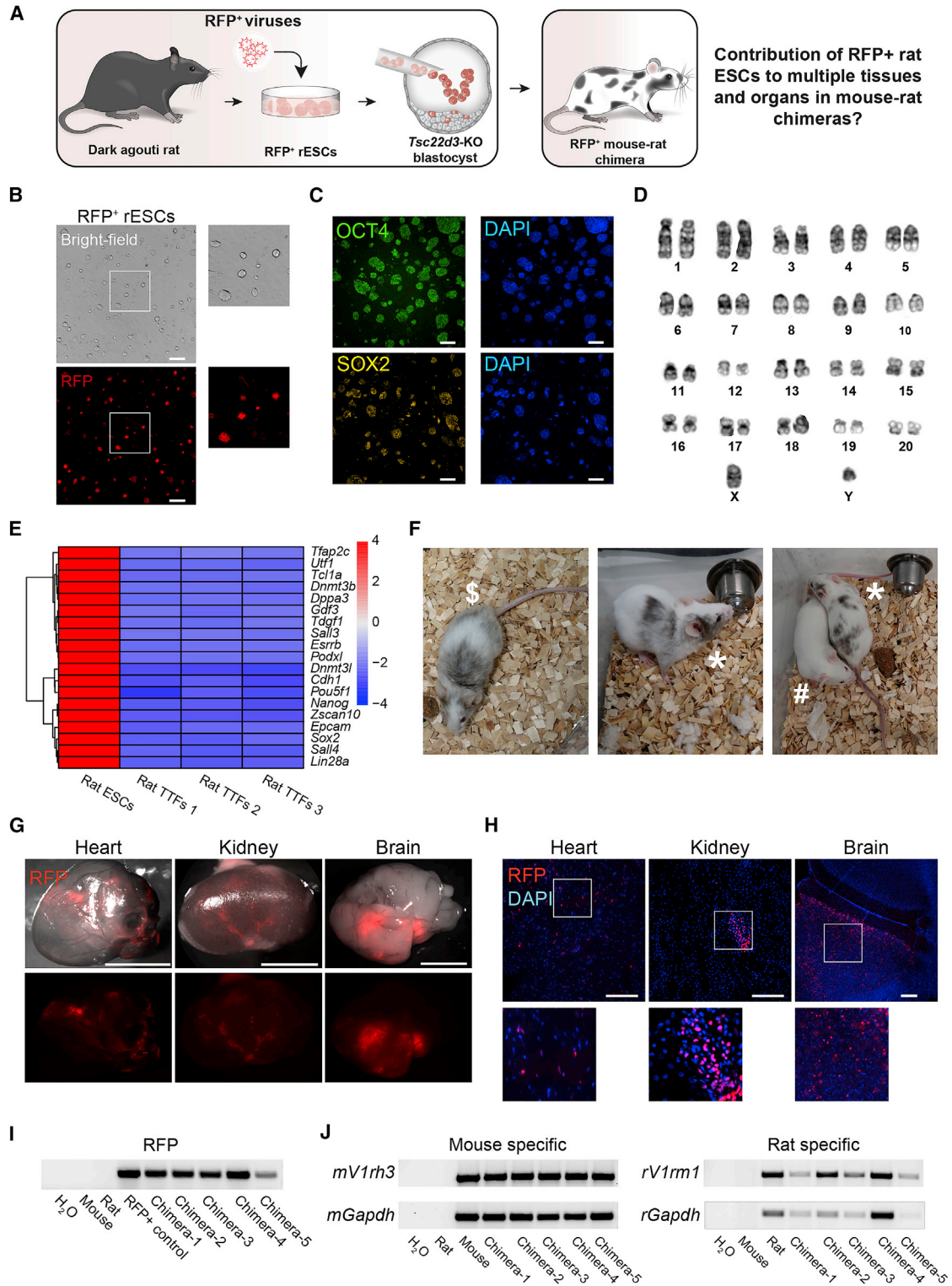


Figure 3. Generation and characterization of mouse-rat chimeras

(A) A schematic illustrating experimental design.

(B) Representative bright-field and RFP images of RFP+DAC8 rESCs. Scale bar, 200 μ m. rESCs, rat embryonic stem cells.

(C) Representative immunofluorescence images of OCT4 and SOX2 in DAC8-rESCs. Scale bar, 200 μ m.

(legend continued on next page)



the germline in comparison with *Pax7-nGFP* iPSCs, as supported by increased contribution of KH2-mESCs to fur color (Figures 1C and 2D). Nonetheless, the *Pax7-nGFP* iPSC/*Tsc22d3*-KO testes that were of bigger size and weight harbored intact seminiferous tubules containing spermatozoa, thus unveiling germline complementation (Figures S2D and S2E). Furthermore, we did not observe TSC22D3 or VASA protein expression in testes harvested from *Tsc22d3*-KO mice, whereas prominent expression of these germ cell-related proteins was documented in testes of a WT mouse and two complemented iPSC-chimeras (Figure 2G). Altogether, out of eight analyzed iPSC-chimeras we detected in the cauda epididymis of three animals mature and motile spermatozoa via percutaneous epididymal sperm aspiration (PESA) procedure or posthumous analysis (Figure S2E, Table S2, and Video S2). To better characterize the cell populations that are present in the cauda epididymis, we performed single-cell RNA sequencing (scRNA-seq) of PESA biopsies extracted from a *Tsc22d3*-KO mouse and a *Pax7-nGFP* iPSC/*Tsc22d3*-KO chimera. This analysis revealed a germ cell population that was only present in the *Pax7-nGFP*-iPSC/*Tsc22d3*-KO chimera and expressed post-meiotic markers indicative of late-stage spermatogenesis such as *Prm1* and *Prm2* (Figures 2H, 2I, and S2F). In contrast, a PESA biopsy of a *Tsc22d3*-KO male mouse was devoid of cells expressing spermatid markers and was mainly composed of immune cells in the form of macrophages and B cells (Figures 2H, 2I, and S2F).

Next, we subjected PESA-derived cells from *Pax7-nGFP* iPSC/*Tsc22d3*-KO chimeras to FACS-purification for haploid cells based on DNA content and isolated mature spermatozoa (Figures S2G and S2H). PCR on genomic DNA extracted from the sorted spermatozoa demonstrated presence of the *Pax7-nGFP* transgenic allele (Figure S2I). Importantly, natural breeding of two complemented chimeras with albino female mice solely produced agouti F1 pups that all carried the *Pax7-nGFP* reporter allele, thus demonstrating the exclusive germline transmission of *Pax7-nGFP* iPSCs (Figures 2J and 2K). Last, FACS-purification of satellite cells from limb muscles of an F1 pup gave rise to a population of proliferative *Pax7-nGFP*⁺ myoblasts that could further differentiate into multinucleated myotubes that were GFP

negative (Figures S2J and S2K). Based on these results, and similar to mESCs, we conclude that transgenic miPSCs can reconstitute the male germline in intraspecies chimeras, giving rise via natural mating to mouse progeny that is exclusively iPSC-derived.

DAC8 rat ESCs contribute to multiple organs and tissues in mouse-rat chimeras

Following the success in restoring fertility via intraspecies blastocyst complementation with mouse PSCs in male chimeras, we next investigated whether injection of rat PSCs into *Tsc22d3*-KO mouse embryos can reconstitute the male germline niche and produce rat spermatozoa in mouse-rat chimeras. To this end, we set out to attempt production of adult mouse-rat chimeras using DAC8 rat ESCs (DAC8-rESCs), a line that was previously shown to contribute to chimerism and germline transmission in rats (Figure 3A) (Li et al., 2008; Tong et al., 2010). As a first step, we transduced DAC8-rESCs with lentiviruses encoding for constitutive H2B-RFP expression followed by FACS-purification of RFP⁺ cells to produce a homogeneous population of RFP⁺DAC8-rESCs for injections (Figures 3A and 3B). DAC8-RFP⁺rESCs expressed pluripotency markers and maintained a normal diploid male karyotype (Figures 3C and 3D). Furthermore, we confirmed via bulk RNA-seq analysis that DAC8-rESCs highly expressed, in comparison with rat fibroblasts, a suite of canonical markers indicative of pluripotency (Figure 3E). To assess the contribution of rESCs to chimerism in mice, we injected 12 to 15 RFP⁺DAC8-rESCs or DAC8-rESCs into *Tsc22d3*-KO blastocysts and transferred the embryos into the oviducts of foster mice. These efforts resulted in production of 16 mouse-rat chimeras as judged by visual inspection of fur color, exhibiting various degrees of coat color chimerism (Figure 3F and Table S3). Of note, we observed lower generation of interspecies mouse-rat chimeras in comparison with intraspecies chimeras, a finding that may be attributed to curtailed contribution of rat ESCs to mouse chimerism or increased embryonic lethality of mouse-rat chimeras as previously reported (Bozyk et al., 2017; Yamaguchi et al., 2018). Importantly, most of the mouse-rat chimeras appeared healthy and developed normally while exhibiting mouse size and weight (Figure S3A). However, a few chimeras

(D) A karyogram of DAC8-rESCs showing a normal set of 42 chromosomes.

(E) A heatmap depicting expression of pluripotency genes based on global RNA-seq of rESCs and three rat TTFs lines. TTFs, tail tip fibroblasts.

(F) Representative photos of three adult mouse-rat chimeras demonstrating dark agouti fur color from the contribution of injected DAC8-rESCs. “#” denotes a non-chimeric *Tsc22d3*-KO mouse, “*” denotes a male mouse-rat chimera, “\$” denotes a female mouse-rat chimera.

(G) Representative bright-field and RFP images of the indicated organs that were harvested from mouse-rat chimeras. Scale bar, 5 mm.

(H) Representative cross-section images of the indicated organs harvested from RFP⁺DAC8-rESCs/*Tsc22d3*-KO chimeras and demonstrating RFP⁺ reporter expression. Scale bar, 100 μ m.

(I) A PCR analysis for presence of the RFP transgene in the indicated animals.

(J) A gel depicting species-specific PCR for mouse (*mV1rh3*, *mGapdh*) or rat (*rV1rm1*, *rGapdh*) genes in the indicated animals.

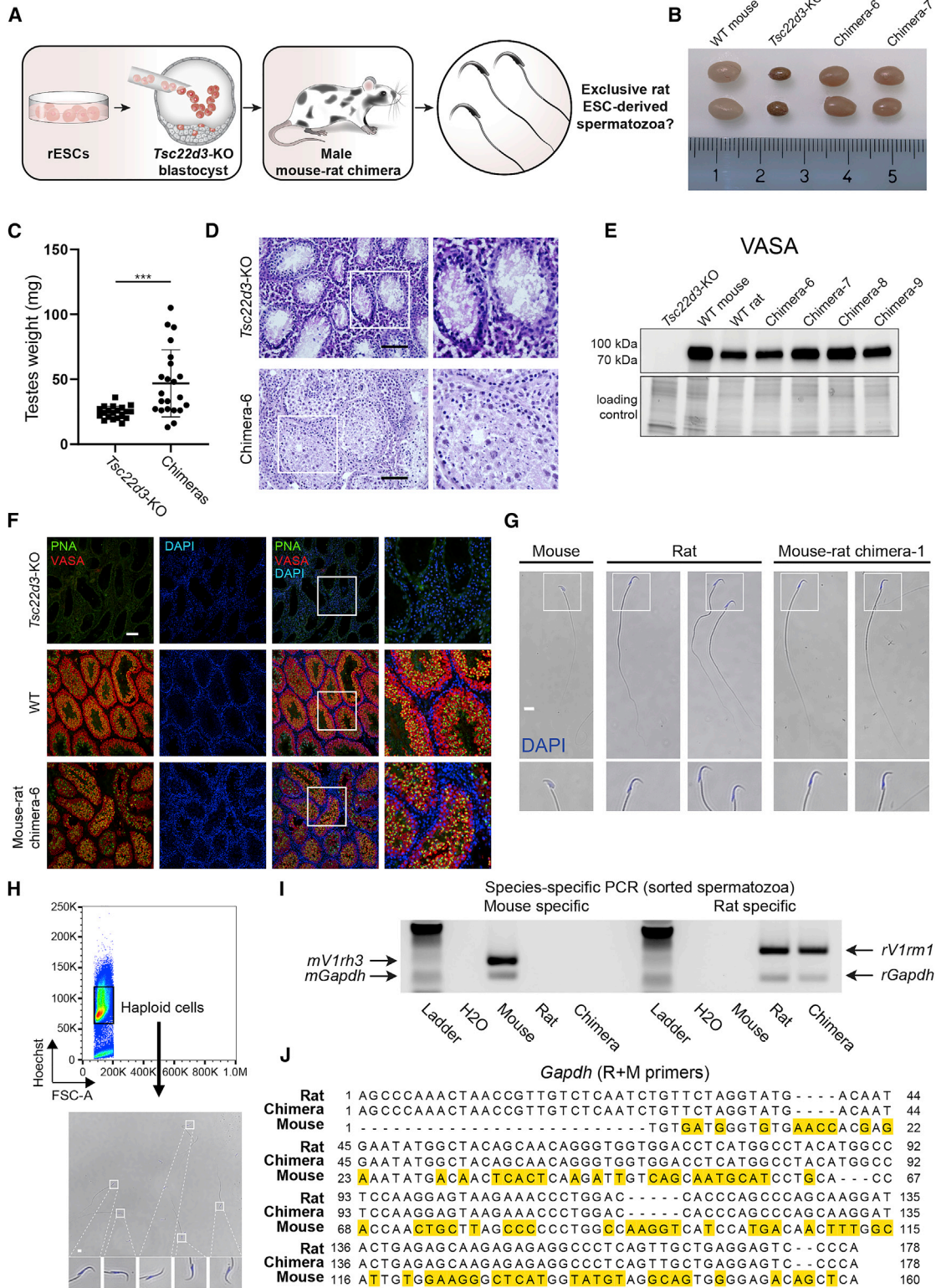


Figure 4. Exclusive generation of rat spermatozoa in mouse-rat chimeras

(A) A schematic illustrating experimental design.

(B) A representative photo of isolated testes from the indicated animals.

(legend continued on next page)



exhibited reduced body size and weight, malocclusion, or other abnormalities as reported by others (Figure S3A) (Bozyk et al., 2017; Yamaguchi et al., 2018). Interestingly, one female mouse-rat chimera had reached over 1 year of age, suggesting that a chimera composed of XY-rat/XX-mouse cells can successfully reach an adult age (Figure 3F). We analyzed several internal organs for RFP expression and detected contribution of RFP⁺DAC8-rESCs to the heart, brain, kidney, and spleen, and further confirmed presence of the RFP transgene (Figures 3G, 3H, 3I, and S3B). We then subjected genomic DNA extracted from skin biopsies of chimeras to species-specific PCR using either mouse- or rat-specific primers and detected both mouse and rat DNA (Figure 3J). Taken together, we show that injection of DAC8-rESCs into *Tsc22d3*-KO blastocysts gave rise to viable mouse-rat chimeras that predominantly appeared normal and could reach adulthood. Contribution of rESCs was detected in the heart and brain, demonstrating a permissive environment for two distinct genotypes to coexist in important organs.

Exclusive production of rESC-derived spermatozoa in interspecies chimeras

Following the success in production of adult mouse-rat chimeras, we next wished to investigate whether DAC8-rESCs or RFP⁺DAC8-rESCs can exclusively give rise to rat spermatozoa in interspecies mouse-rat chimeras (Figure 4A). To this end, we euthanized and posthumously inspected an RFP⁺DAC8-rESC high-grade mouse-rat chimera-1 and documented large testicular size in comparison with a non-complemented *Tsc22d3*-KO control (Figures S4A and S4B). Large testicular size was also observed in several other DAC8-rESC/*Tsc22d3*-KO chimeras (Figures 4B and 4C). A testis cross-section of mouse-rat chimera-1 showed strong nuclear RFP expression, emanating from RFP⁺DAC8-rESCs (Figure S4C). Most notably, testes of *Tsc22d3*-KO mice exhibited atrophic seminiferous tubules, whereas testes of several mouse-rat chimera demonstrated intact tubules containing spermatozoa (Figure 4D). We further detected presence of the germ cell and spermatid-associated proteins VASA and PNA in the testes of several DAC8-rESC/*Tsc22d3*-

KO chimeras, whereas these germ cell markers were absent in the testes of *Tsc22d3*-KO mice (Figures 4E and 4F).

Immature spermatozoa gain motility and fertilization capacity as they transition from the testes through the epididymis, where they are stored in the cauda epididymis (Gervasi and Visconti, 2017). Spermatozoa extracted from the cauda epididymis of 2- to 3-month old mouse-rat chimeras contained elongated tails with a typical rat sperm head-morphology, whereas no spermatozoa were detected in the cauda epididymis of *Tsc22d3*-KO mice (Figures 4G and S4D). However, these spermatozoa were immotile, and we further detected in the cauda epididymis immature elongated spermatids containing intact tails albeit lacking the typical sperm head-morphology associated with mature rat spermatozoa (Figure S4D). To unequivocally confirm exclusive contribution of rESCs to the production of rat spermatozoa in mouse-rat chimeras, we subjected cells that were extracted from the cauda epididymis of mouse-rat chimera-1 to FACS-purification for haploid cells based on DNA content (Figure 4H). Using this method, we purified spermatozoa containing elongated tails and typical rat sperm head-morphology indicative of mature spermatozoa (Figure 4H). We then extracted genomic DNA from these spermatozoa and subjected it to species-specific PCR for the mouse and rat *Gapdh* and vomeronasal receptor genes (mouse *V1rh3* or rat *V1rm1*). We could only detect rat *Gapdh* and *V1rm1* PCR bands in the FACS-purified spermatozoa, and no PCR bands for mouse genes were detected (Figure 4I). Next, we subjected the PCR products to sequencing and documented complete matched read alignment only with the rat reference genome (Figures 4J and S4E). Collectively, these findings demonstrate that rESCs can overcome the germline differentiation defect attributed to lack of the TSC22D3 protein in sterile mice and exclusively produce haploid rat spermatozoa in interspecies chimeras.

Characterization of cell types and differentiation trajectory in a mouse-rat chimera testis by scRNA-seq

Our observation that rat germ cells can be produced in the testes of mouse-rat chimeras prompted us to investigate to

(C) Quantification of testes weight in the indicated animals (n = 20–22 biological replicates; each dot represents a single testis, unpaired two tailed t test was used, error bars denote SD, ***p < 0.001).

(D) H&E staining of testes cross-sections from the indicated samples. Scale bar, 100 μ m.

(E) Western blot analysis for VASA protein expression in the indicated testes samples.

(F) Immunostaining for VASA and PNA in testes of the indicated animals. Scale bar, 100 μ m.

(G) Representative images of spermatozoa extracted from the cauda epididymis of the indicated animals and counterstained with DAPI. Scale bar, 10 μ m.

(H) FACS-sorting strategy for purification of haploid cells from the cauda epididymis of RFP⁺DAC8rESCs/*Tsc22d3*-KO mouse-rat chimera-1. Shown is a representative image of sorted spermatozoa embodying rat sperm head-morphology. Scale bar, 10 μ m.

(I) A gel showing species-specific PCR for the indicated genes in haploid spermatozoa sorted from the cauda epididymis of the indicated animals.

(J) DNA sequencing of the mouse and rat *Gapdh* PCR products shown in Figure 4I. Misalignments are highlighted in yellow.

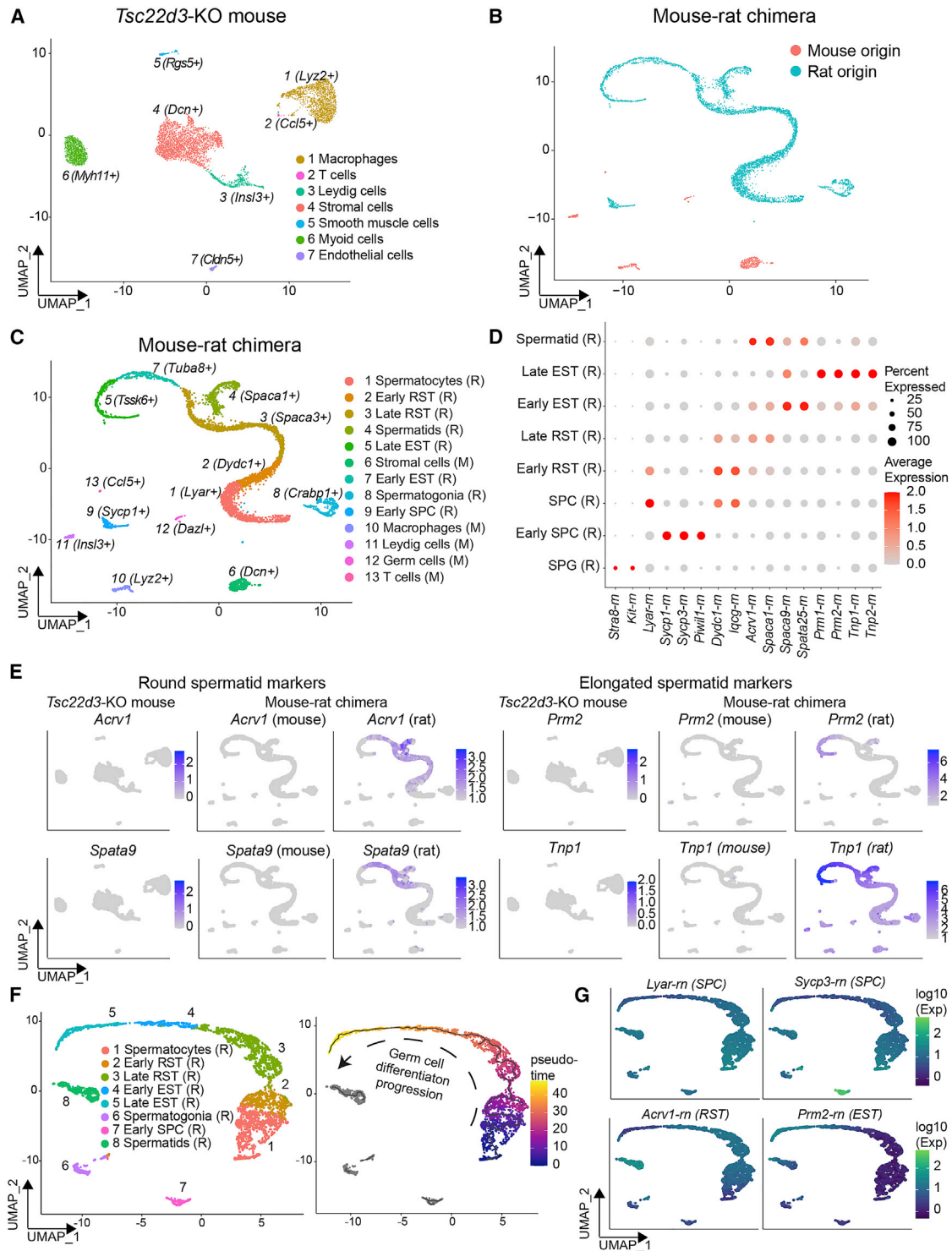


Figure 5. scRNA-seq of testicular cells derived from a germline-complemented mouse-rat chimera

(A) UMAP projection of *Tsc22d3*-KO testis representing 6,382 cells and colored by different cell types. Note absence of germ cells.

(B) UMAP projection of mouse-rat chimera testis representing 5,060 cells colored by species.

(C) UMAP projection based on scRNA-seq data of a mouse-rat chimera testis representing 5,060 cells colored by different cell types. R, Rat; M, Mouse; RST, round spermatids; EST, elongated spermatids; SPC, spermatocytes.

(legend continued on next page)



what extent rat cells undergo spermatogenesis in a xenogeneic environment lacking a TSC22D3 protein. To this end, we performed scRNA-seq of testes from a *Tsc22d3*-KO mouse and a mouse-rat chimera. Expectedly, the *Tsc22d3*-KO testis was devoid of germ cells yet consisted of white blood, endothelial, and Leydig cells (Figure 5A). Further, as we expected to find cells of both rat and mouse origin in a chimera testis, we created a custom mouse-rat chimera reference genome and mapped both samples against it to ensure species specificity. Mapping results demonstrated that the *Tsc22d3*-KO testis was only composed of mouse cells, whereas the chimera testis contained cells expressing either mouse or rat genes, albeit predominantly the latter (Figures 5B and S5A). Mouse cell populations in a chimera testis consisted of white blood, stromal, and Leydig cells in addition to a very small population of pre-meiotic germ cells, which presumably indicate an early cell population preceding the differentiation blockage inflicted by the *Tsc22d3* mutation (Figure 5C). In stark contrast, rat cells in the chimera testis were annotated as spermatogonial cells (*Crabp1*⁺, *Uchl1*⁺), spermatocytes (*Sycp3*⁺, *Piwil1*⁺), round spermatids (*Acrv1*⁺, *Spaca1*⁺), and elongated spermatids (*Tnp1*⁺, *Prm2*⁺), thus representing multiple differentiation stages of spermatogenesis (Figures 5C and 5D). Interestingly, only germ cells yet no other somatic cell type was of rat origin, suggesting a preferential contribution of rat PSCs toward the germline in the chimera testis (Figure 5C). Further, a cell cycle analysis demonstrated that rat spermatogonia and spermatocytes are predominantly in an S and G2/M proliferation state, whereas downstream cell types gradually exited the cell cycle as they transitioned through meiosis and underwent terminal differentiation into elongated spermatids (Figure S5B). Examination of various markers for spermatogenesis revealed that none of the inspected genes were expressed in a *Tsc22d3*-KO mouse testis and only rat germ cell transcripts were expressed in a chimera testis (Figures 5D, 5E, and S5C). In addition, we documented a similar pattern of rat germ cells in a chimera testis and a WT rat testis, confirming high expression of genes such as *Prm1*, *Tnp2*, and *Tssk6* that are indicative of late elongated spermatids in both samples (Figure S5C).

Next, we performed a pseudotime lineage trajectory analysis for rat cells and confirmed the progression from spermatocytes to round and elongated spermatids in a

chimera testis (Figure 5F). Of note, we also detected spermatogonia, spermatocytes, and spermatid cell populations that did not participate in the lineage trajectory (Figure 5F). Based on the trajectory analysis, we observed a pseudotime difference within round and elongated spermatid populations, indicating that these populations are composed of cells representing different stages of spermatogenesis (Figure 5G). We annotated the stages into early and late based on the high expression of well-established markers (Figures 5G and S5D). To conclude, the scRNA-seq unequivocally determined that only rat cells participate in spermatogenesis in a mouse-rat chimera testis harboring a *Tsc22d3* mutation. This analysis helped to dissect the various rat cell types undergoing germline differentiation in a xenogeneic mouse host environment, and further highlighted several rat germ cell populations that did not participate in the differentiation trajectory.

Fertilization of rat oocytes with interspecies rat spermatozoa

The exclusive production of rat germ cells in interspecies chimeras raised the question whether these cells can fertilize rat oocytes. As mouse-rat chimeras are of mouse size and might be preyed on by rats, we opted to use Intracytoplasmic Sperm Injection (ICSI), an assisted reproductive technology, to attempt fertilization of rat oocytes (Hirabayashi et al., 2002). We first trialed generation of rats using frozen-thawed cauda-derived spermatozoa produced in rats (Figure 6A). We were successful in generating live and healthy rat progeny via ICSI and in addition could grow fertilized zygotes to the blastocyst stage *in vitro* (Figure 6B). As the next step, we trialed injection of frozen-thawed cauda epididymis-derived spermatozoa from an interspecies chimera into Sprague-Dawley (SD) rat oocytes (Figure 6C). To this end, we injected spermatozoa that were produced in mouse-rat chimera-1. We first attempted production of embryos *in vitro* to determine if interspecies rat spermatozoa can support early-stage embryonic development. We performed ICSI with 312 SD oocytes, out of which 213 embryos survived, resulting in several rat embryos that developed until 4- to 8-cell stage, in addition to morula and blastocyst-stage embryos (Figures 6D and 6E). Of note, the rate of embryo production was substantially lower in comparison with similar *in vitro* trials conducted with rat spermatozoa produced in rats (Figure 6B).

(D) Dot plot for individual gene expression in various germ cell populations as shown in Figure 3C. rn, *Rattus norvegicus*; SPG, spermatogonia.

(E) UMAP projection of *Tsc22d3*-KO and mouse-rat chimera testes showing all cells colored by the expression level of the indicated spermatid markers.

(F) Monocle3 UMAP projection showing all rat cells ($n = 4,491$) from a mouse-rat chimera colored by different cell types (left) and calculated pseudotime values (right).

(G) Monocle3 UMAP projection showing all rat cells from a mouse-rat chimera colored by the expression level of the indicated germ cell markers.

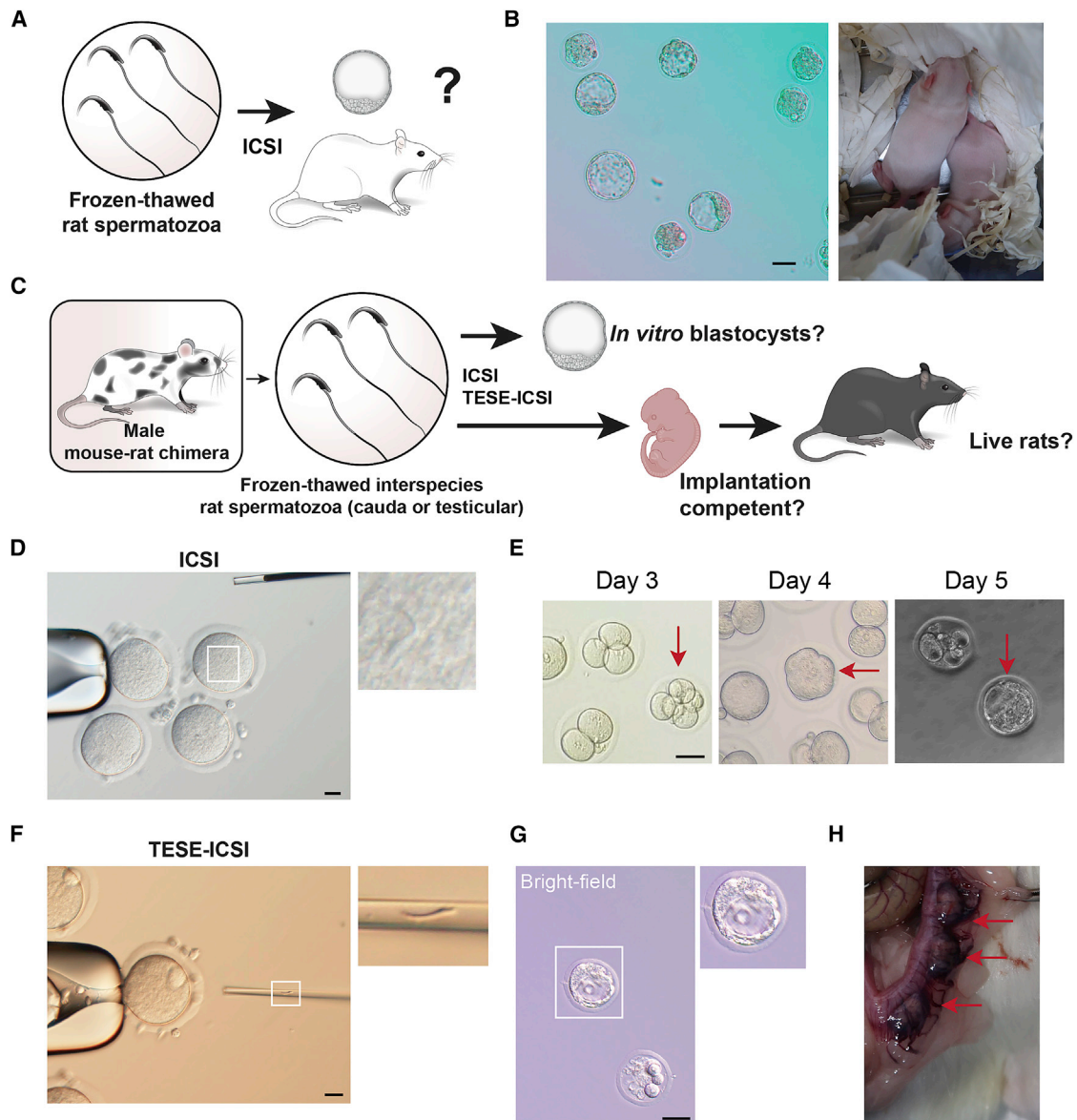


Figure 6. Fertilization of rat oocytes with rat spermatozoa exclusively produced in interspecies chimeras

(A) A schematic illustrating experimental design.

(B) Blastocysts generated via ICSI from cauda epididymis-derived spermatozoa produced in rats (left) and derivative pups (right). Scale bar, 50 μm . ICSI, intracytoplasmic sperm injection.

(C) A schematic illustrating experimental design. TESE-ICSI, Testicular Sperm Extraction ICSI.

(D) Rat oocytes injected with cauda epididymis-derived spermatozoa produced in mouse-rat chimera-1 via ICSI. Scale bar, 20 μm .

(E) Images showing rat embryos produced from interspecies rat spermatozoa of mouse-rat chimera-1. Frozen-thawed cells were injected into rat Sprague-Dawley (SD) oocytes via ICSI and cultured *in vitro*. Shown are 4- to 8-cell stage, morula-stage and blastocyst-stage rat embryos at the indicated days, as pointed by arrows. Scale bar, 50 μm .

(F) Image depicting an interspecies testicular rat germ cell prior to injection into an SD oocyte. Scale bar, 20 μm .

(G) An image showing a blastocyst that was generated using an interspecies rat germ cell from the testes of a GFP⁺ mouse-rat chimera. Frozen-thawed cells were injected into SD oocytes via TESE-ICSI and cultured *in vitro*. Scale bar, 50 μm .

(H) A photo showing three embryonic implantation sites in a foster female after embryo transfer of SD oocytes injected with mouse-rat chimera germ cells. Arrows point to implantation sites.



Next, to attempt generation of adult rats, 239 SD oocytes were injected with interspecies spermatozoa from chimera-1 and 180 embryos were transferred into the oviducts of foster SD rats; however, did not produce live rats.

Due to the inability to produce live rats from cauda epididymis-derived spermatozoa of a mouse-rat chimera, we reasoned that germ cells at an earlier developmental stage might produce rats via Testicular Sperm Extraction (TESE)-ICSI (Isotani et al., 2016) (Figure 6C). To investigate this hypothesis, we generated new interspecies chimeras by injection of *Tsc22d3*-KO blastocysts with *F344-Tg.EC4011/Rrrc* rESCs, which are heterozygous for a ubiquitin C promoter-EGFP (*UBC-EGFP*) transgene and were previously shown to contribute to germline transmission in rats (Lois et al., 2002; Men and Bryda, 2013). Similar to DAC8-rESCs, *UBC-EGFP* rESCs could contribute to chimerism in mice and produce interspecies chimeras of normal mouse body weight (Figure S6A). Notably, two *UBC-EGFP*-rESC/*Tsc22d3*-KO mouse-rat chimeras exhibited significantly larger testes in comparison with *Tsc22d3*-KO mice and expressed the EGFP transgene (Figures S6B–S6E). We dissociated the EGFP⁺ testes posthumously and detected multiple spermatozoa showing typical rat sperm head-morphology in the testes of one chimera (Figure S6F). We then performed TESE-ICSI with 208 oocytes, out of which 136 survived, with frozen-thawed interspecies testicular germ cells derived from an EGFP⁺ mouse-rat chimera. This trial gave rise to an EGFP⁺ blastocyst upon *in vitro* embryo culture (Figures 6G and S6G). Notably, transfer of 113 embryos (194 injected) into foster mothers did not produce live rats. Last, as we did not document rat births, we decided to investigate whether blastocysts can be produced *in vivo* and implant into the uterus (Figure 6C). To this end, we performed a C-section of foster mothers, which were subjected to embryo transfer with one or two cell-stage embryos (206 embryos in total). Surprisingly, we detected several implantation sites containing resorbed embryos, and one expressing the EGFP reporter (Figures 6H and S6H). In summary, frozen-thawed germ cells from the two examined interspecies chimeras contained cells that carry potential to fertilize rat oocytes and give rise to blastocysts *in vitro*, or implanted embryos that resorbed; however, not to live rats.

DISCUSSION

In this study we report on a method to exclusively produce germ cells of one species in another by using blastocyst complementation with PSCs. Capitalizing on the sterility-associated mutation in *Tsc22d3*-KO mouse blastocysts, we documented production of intraspecies and interspecies chimeras that embody mouse or rat spermatozoa solely from injected ESCs or iPSCs. Notably, mouse intraspecies

chimeras harboring PSC-derived spermatozoa solely gave rise to PSC-derived adult mice, whereas interspecies rat spermatozoa could fertilize oocytes and produce blastocysts and implantation-competent embryos. However, for the two examined mouse-rat chimeras, embryos fertilized with frozen-thawed interspecies germ cells did not develop normally, and live births were not recorded.

In general, the capacity to produce interspecies chimeras with somatic and germline contribution is expected to be dependent on species similarity and a physiologically receptive environment that is permissive for two distinct genotypes to coalesce in the same organism, as demonstrated in recent years for adult or fetal mouse-rat, human-monkey, and human-pig chimeras (Das et al., 2020; Maeng et al., 2021; Tan et al., 2021; Zheng et al., 2021a). Furthermore, contribution to interspecies chimerism is highly dependent on cell competition and the capacity of PSCs to overcome evolutionary barriers (Ballard and Wu, 2021). Recent efforts to overcome such barriers have been reported and include injection of *TP53*, *Myd88*-or *P65*-null PSCs, overexpression of the anti-apoptotic gene *Bcl2* in PSCs or harnessing mouse *Igf1r*-null blastocysts to increase contribution of PSCs to chimerism (Maeng et al., 2021; Masaki et al., 2016; Nishimura et al., 2021; Zheng et al., 2021b). With respect to germline complementation, given that we documented a relatively low number of interspecies chimera production, we postulate that using such methods may augment the capacity of PSCs to contribute to chimerism and in particular to the germline. However, such methods also warrant caution, as production of chimeras with extensive contribution from xenogeneic PSCs could be detrimental to survival during embryonic development (Bozyk et al., 2017; Yamaguchi et al., 2018).

To date, interspecies blastocyst complementation between a mouse and a rat has been documented for various organs and tissues, including pancreas, thymus, kidney, and blood vasculature (Goto et al., 2019; Isotani et al., 2011; Kobayashi et al., 2010; Wang et al., 2020; Wu et al., 2017; Yamaguchi et al., 2017; Zheng et al., 2021a). With respect to contribution of rat PSCs to the germline in mice, two studies previously reported on the production of functional rat spermatozoa in mouse-rat chimeras from injected rESCs or riPSCs (Isotani et al., 2016; Tsukiyama et al., 2014). However, chimera testes contained both mouse and rat spermatozoa, necessitating a genetic reporter or morphological examination to distinguish between the two cell types (Isotani et al., 2016; Tsukiyama et al., 2014). The capacity to solely generate rat spermatozoa in sterile mice renders use of such methods potentially dispensable. Moreover, in agreement with our findings, a recent study by Kobayashi and colleagues documented germline blastocyst complementation in rats using embryos that carry a mutation in *Prdm14*, an essential gene for germ cell production (Kobayashi et al., 2020, 2021;



Yamaji et al., 2008). The authors further demonstrated interspecies blastocyst complementation via injection of mouse PSCs into *Prdm14*-KO rat embryos, solely generating functional mouse spermatids in rats that could give rise to live mice via Round Spermatid Injection (ROSI) (Kobayashi et al., 2021). The findings reported in that study, and the results reported herein, synergize to suggest that both mouse and rat PSCs can complement the male germline in interspecies chimeras by injection into blastocysts that carry mutations that preclude spermatogenesis. Furthermore, these and other observations suggest that mutations in different essential genes for germ cell production provide a vacant niche receptive for reconstitution with PSCs (Kobayashi et al., 2021; Koentgen et al., 2016; Miura et al., 2021; Taft et al., 2013).

Our efforts to produce live rats from frozen-thawed interspecies spermatozoa produced in two mouse-rat chimeras were unsuccessful. We hypothesize two reasons that may account for this result: (1) Effect of cell freezing: the ICSI and TESE-ICSI trials reported in this study were performed using frozen-thawed cauda epididymis or testicular germ cells. We speculate that use of non-frozen germ cells may carry increased chances of fertilization by mitigating potential impairment due to freeze-thaw cycles. (2) Impaired interspecies germ cells: rat spermatogonia subjected to differentiation in mouse testes encounter a xenogeneic environment that is receptive toward differentiation of mouse and not rat cells, potentially impairing the functionality of interspecies rat germ cells. In support of this hypothesis, we documented via scRNA-seq several rat germ cell populations in a chimera testis that did not participate in the lineage differentiation progression toward an elongated spermatid cell population, potentially indicating an impaired process. To address this limitation, using immature germ cells via ROSI may lend a more favorable technique for production of animals from interspecies germ cells. Indeed, generation of live mice from mouse round spermatids produced in *Prdm14*-KO rats via ROSI was recently reported (Kobayashi et al., 2021). Nonetheless, further work is certainly required to explore the molecular and functional nature of rat germ cells produced in a xenogeneic mouse host in comparison with rat germ cells produced in rats. In particular, it will be of interest to assess whether contribution of rat PSCs to spermatogenesis support cells in the form of Sertoli or Leydig cells will increase the portion of functional interspecies spermatozoa.

Given future experimental success, two additional implications may emanate from our study. The first involves production of rat transgenic models via sterile mice. Rats are commonly used as an animal model for human diseases in biomedical research; however, production of transgenic rats from genetically modified PSCs are oftentimes challenged by low germline transmission rates. As such, the ca-

capacity to use sterile mice as hosts for genetically modified rat PSCs may assist in generation of transgenic rats via a one-step and faster solution (Isotani et al., 2016). This approach is particularly attractive for models that cannot rely on genome engineering tools such as CRISPR-Cas9 to produce transgenic rats, namely insertion of large DNA fragments or an artificial chromosome (Kobayashi et al., 2021). Last, an additional potential implication of this study may extend to animal conservation efforts, as the technique reported herein can be adapted to produce xenogeneic germ cells of endangered animal species. Notably, however, blastocyst complementation of the germline has mostly been trialed thus far for mouse and rat PSCs, whose culture conditions and propensity to contribute to chimerism and the germline are well-established. To assess whether this technique can be adapted to other animal species, generation of additional mammalian PSCs with germline transmission competency is warranted. With success, we envision that germline blastocyst complementation may provide a useful tool to generate germ cells *in vivo* for production of transgenic animal models, or potentially assisting in the preservation efforts of endangered species.

EXPERIMENTAL PROCEDURES

Details on methods, reagents, multiomics analyses, reprogramming, and transgenic techniques can be found in the [supplemental information](#).

Animal strains and cell lines used in this study

The following mouse and rat strains were used in this study: KH2-ESCs, a subclone of V6.5 ESCs derived from a cross between C57BL/6 X 129/sv mice (a kind gift from Dr. Konrad Hochedlinger) (Beard et al., 2006). *Pax7-nGFP* MEFs were derived from *Tg:Pax7-nGFP/C57BL6;DBA2* mice (a kind gift from Dr. Shahragim Tajbakhsh) (Sambasivan et al., 2009). *Tsc22D3*-KO male embryos, also known as “GoGermline” were purchased from Ozgene (Ozgene, Perth, Australia). Rat DAC8-ESCs were derived from a *DA/OlaHsd-ES8/Qly* rat strain (Li et al., 2008) and UBC-GFP ESCs were derived from a *F344-Tg(UBC-EGFP)F455Rrrc* rat strain (Men and Bryda, 2013), and both were purchased from the Rat Resource and Research Center (RRRC) (<https://www.rrrc.us>). Animals were housed in Allentown cages in standard laboratory conditions, room temperature 23°C; relative humidity 50% to 60%; 12:12-h light-dark cycle. Photos of chimeras were taken with Canon PowerShot G7 X Mark II camera. The present study was approved by the Federal Food Safety and Veterinary Office, Cantonal veterinary office (Zurich) and granted animal experiment license numbers ZH124/19 and FormG-135.

Data and code availability

The bulk and scRNA-seq datasets generated in this study are available in the Gene Expression Omnibus (GEO) repository under accession number GSE167435.



SUPPLEMENTAL INFORMATION

Supplemental information can be found online at <https://doi.org/10.1016/j.stemcr.2022.07.005>.

AUTHOR CONTRIBUTIONS

J.Z. and O.B.-N. conceptualized the experiments, interpreted the results, and wrote the manuscript. J.Z. performed most experiments and analysis of results. O.B.-N. supervised the study. M.T.-S. helped with experiments involving chimera production and performed the PESA, blastocyst injection, embryo transfer, ICSI, and TESE-ICSI procedures. A.G. oversaw the generation of bulk mRNA-seq and scRNA-seq data in addition to analysis and interpretation of results and manuscript writing. N.B. assisted with FACS, H&E staining, PCR analysis, karyotype preparation, and lentiviral production. F.N. created the mouse-rat chimeric reference genome, P.G. helped to produce interspecies chimeras, X.Q. performed Western blots, S.D. helped with isolation of myoblasts and performed the *in vitro* differentiation of myoblasts, and I.K. helped to perform immunofluorescence of testes cross-sections. T.H. oversaw the IVF and injection of PSCs in the ETH Phenomics Center at ETH Zurich and helped with interpretation of results. F.v.M., L.H., and C.T. helped to conceptualize the single-cell RNA sequencing experiments, assisted in its execution and helped in result interpretation and manuscript writing.

ACKNOWLEDGMENTS

We thank Dr. Konrad Hochedlinger, Dr. Bruno Di Stefano, and Dr. Justin Brumbaugh, as well as members of the Regenerative and Movement Biology Laboratory for their constructive comments and feedback. We are grateful to Dr. Shahragim Tajbakhsh for providing the *Pax7-mGFP* mouse strain and Dr. Konrad Hochedlinger for providing the KH2-ESCs, *M2rtTA*, and *STEMCCA* lentiviral cassettes. We further thank Dr. Hongsheng Men and Dr. Elizabeth Bryda from the Rat Resource and Research Center (RRRC) at the University of Missouri for their valuable suggestions with respect to rat embryo culture, DNA sequencing, and ICSI. We are also grateful to the staff members at the EPIC transgenic core in the ETH Phenomics center of ETH Zurich for their help with a portion of the injections. We acknowledge the use of the Functional Genomics Center Zurich (FGCZ) and are grateful to their staff members for their assistance with next generation library preparation and Illumina sequencing of mRNA and scRNA samples. We also thank SciArtWork for their help with preparation of graphical images, whereas a few other graphical schematics were also created with BioRender.com. This work was supported by startup funds from ETH Zurich to O. Bar-Nur. Other support to the Bar-Nur group includes an Eccellenza grant from the Swiss National Science Foundation (grant no. PCEGP3_187009) as well as grants from The Good Food Institute Foundation, The Novartis Foundation for Medical-Biological Research, The Helmut Horten Foundation and NCCR Robotics (grant number 51NF40_185543). Work in the von Meyenn group is supported by the European Research Council (ERC) under the European Union's Horizon 2020 research and innovation program (grant agreement no. 803491).

CONFLICTS OF INTEREST

The authors declare no competing interests.

Received: May 31, 2022

Revised: July 6, 2022

Accepted: July 7, 2022

Published: August 4, 2022

REFERENCES

- Ballard, E.B., and Wu, J. (2021). Growth competition in interspecies chimeras: a new paradigm for blastocyst complementation. *Cell Stem Cell* 28, 3–5.
- Bar-Nur, O., Brumbaugh, J., Verheul, C., Apostolou, E., Pruteanu-Malinici, I., Walsh, R.M., Ramaswamy, S., and Hochedlinger, K. (2014). Small molecules facilitate rapid and synchronous iPSC generation. *Nat. Methods* 11, 1170–1176.
- Beard, C., Hochedlinger, K., Plath, K., Wutz, A., and Jaenisch, R. (2006). Efficient method to generate single-copy transgenic mice by site-specific integration in embryonic stem cells. *Genesis* 44, 23–28.
- Bozyk, K., Gilecka, K., Humiecka, M., Szpila, M., Suwinska, A., and Tarkowski, A.K. (2017). Mouse↔rat aggregation chimaeras can develop to adulthood. *Dev. Biol.* 427, 106–120.
- Bruscoli, S., Velardi, E., Di Sante, M., Bereshchenko, O., Venanzi, A., Coppo, M., Berno, V., Mameli, M.G., Colella, R., Cavaliere, A., and Riccardi, C. (2012). Long glucocorticoid-induced leucine zipper (L-GILZ) protein interacts with ras protein pathway and contributes to spermatogenesis control. *J. Biol. Chem.* 287, 1242–1251.
- Chang, A.N., Liang, Z., Dai, H.Q., Chapdelaine-Williams, A.M., Andrews, N., Bronson, R.T., Schwer, B., and Alt, F.W. (2018). Neural blastocyst complementation enables mouse forebrain organogenesis. *Nature* 563, 126–130.
- Chen, J., Gorman, J.R., Stewart, V., Williams, B., Jacks, T., and Alt, F.W. (1993a). Generation of normal lymphocyte populations by Rb-deficient embryonic stem cells. *Curr. Biol.* 3, 405–413.
- Chen, J., Lansford, R., Stewart, V., Young, F., and Alt, F.W. (1993b). RAG-2-deficient blastocyst complementation: an assay of gene function in lymphocyte development. *Proc. Natl. Acad. Sci. USA* 90, 4528–4532.
- Chubb, R., Oh, J., Riley, A.K., Kimura, T., Wu, S.M., and Wu, J.Y. (2017). Vivo rescue of the hematopoietic niche by pluripotent stem cell complementation of defective osteoblast compartments. *Stem Cell.* 35, 2150–2159.
- Das, S., Koyano-Nakagawa, N., Gafni, O., Maeng, G., Singh, B.N., Rasmussen, T., Pan, X., Choi, K.D., Mickelson, D., Gong, W., et al. (2020). Generation of human endothelium in pig embryos deficient in ETV2. *Nat. Biotechnol.* 38, 297–302.
- Gervasi, M.G., and Visconti, P.E. (2017). Molecular changes and signaling events occurring in spermatozoa during epididymal maturation. *Andrology* 5, 204–218.
- Goto, T., Hara, H., Sanbo, M., Masaki, H., Sato, H., Yamaguchi, T., Hochi, S., Kobayashi, T., Nakauchi, H., and Hirabayashi, M.



- (2019). Generation of pluripotent stem cell-derived mouse kidneys in Sall1-targeted anephric rats. *Nat. Commun.* *10*, 451.
- Hamanaka, S., Umino, A., Sato, H., Hayama, T., Yanagida, A., Mizuno, N., Kobayashi, T., Kasai, M., Suchy, F.P., Yamazaki, S., et al. (2018). Generation of vascular endothelial cells and hematopoietic cells by blastocyst complementation. *Stem Cell Rep.* *11*, 988–997.
- Hirabayashi, M., Kato, M., Aoto, T., Sekimoto, A., Ueda, M., Miyoshi, I., Kasai, N., and Hoshi, S. (2002). Offspring derived from intracytoplasmic injection of transgenic rat sperm. *Transgenic Res.* *11*, 221–228.
- Isotani, A., Hatayama, H., Kaseda, K., Ikawa, M., and Okabe, M. (2011). Formation of a thymus from rat ES cells in xenogeneic nude mouse ↔ rat ES chimeras. *Gene Cell.* *16*, 397–405.
- Isotani, A., Yamagata, K., Okabe, M., and Ikawa, M. (2016). Generation of Hprt-disrupted rat through mouse ← rat ES chimeras. *Sci. Rep.* *6*, 24215.
- Kitahara, A., Ran, Q., Oda, K., Yasue, A., Abe, M., Ye, X., Sasaoka, T., Tsuchida, M., Sakimura, K., Ajioka, Y., et al. (2020). Generation of lungs by blastocyst complementation in apneumatic Fgf10-deficient mice. *Cell Rep.* *31*, 107626.
- Kobayashi, T., Yamaguchi, T., Hamanaka, S., Kato-Itoh, M., Yamazaki, Y., Ibata, M., Sato, H., Lee, Y.S., Usui, J.I., Knisely, A.S., et al. (2010). Generation of rat pancreas in mouse by interspecific blastocyst injection of pluripotent stem cells. *Cell* *142*, 787–799.
- Kobayashi, T., Kobayashi, H., Goto, T., Takashima, T., Oikawa, M., Ikeda, H., Terada, R., Yoshida, F., Sanbo, M., Nakauchi, H., et al. (2020). Germline development in rat revealed by visualization and deletion of Prdm14. *Development* *147*, dev183798.
- Kobayashi, T., Goto, T., Oikawa, M., Sanbo, M., Yoshida, F., Terada, R., Niizeki, N., Kajitani, N., Kazuki, K., Kazuki, Y., et al. (2021). Blastocyst complementation using Prdm14-deficient rats enables efficient germline transmission and generation of functional mouse spermatids in rats. *Nat. Commun.* *12*, 1328.
- Koentgen, F., Lin, J., Katidou, M., Chang, I., Khan, M., Watts, J., and Lombaerts, P. (2016). Exclusive transmission of the embryonic stem cell-derived genome through the mouse germline. *Genesis* *54*, 326–333.
- Li, P., Tong, C., Mehrian-Shai, R., Jia, L., Wu, N., Yan, Y., Maxson, R.E., Schulze, E.N., Song, H., Hsieh, C.L., et al. (2008). Germline competent embryonic stem cells derived from rat blastocysts. *Cell* *135*, 1299–1310.
- Lois, C., Hong, E.J., Pease, S., Brown, E.J., and Baltimore, D. (2002). Germline transmission and tissue-specific expression of transgenes delivered by lentiviral vectors. *Science* *295*, 868–872.
- Maeng, G., Das, S., Greising, S.M., Gong, W., Singh, B.N., Kren, S., Mickelson, D., Skie, E., Gafni, O., Sorensen, J.R., et al. (2021). Humanized skeletal muscle in MYF5/MYOD/MYF6-null pig embryos. *Nat. Biomed. Eng.* *5*, 805–814.
- Masaki, H., Kato-Itoh, M., Takahashi, Y., Umino, A., Sato, H., Ito, K., Yanagida, A., Nishimura, T., Yamaguchi, T., Hirabayashi, M., et al. (2016). Inhibition of apoptosis overcomes stage-related compatibility barriers to chimera formation in mouse embryos. *Cell Stem Cell* *19*, 587–592.
- Matsunari, H., Nagashima, H., Watanabe, M., Umeyama, K., Nakano, K., Nagaya, M., Kobayashi, T., Yamaguchi, T., Sumazaki, R., Herzenberg, L.A., and Nakauchi, H. (2013). Blastocyst complementation generates exogenic pancreas in vivo in apantecric cloned pigs. *Proc. Natl. Acad. Sci. USA.* *110*, 4557–4562.
- Matsunari, H., Watanabe, M., Hasegawa, K., Uchikura, A., Nakano, K., Umeyama, K., Masaki, H., Hamanaka, S., Yamaguchi, T., Nagaya, M., et al. (2020). Compensation of disabled organogenesis in genetically modified pig fetuses by blastocyst complementation. *Stem Cell Rep.* *14*, 21–33.
- Men, H., and Bryda, E.C. (2013). Derivation of a germline competent transgenic Fischer 344 embryonic stem cell line. *PLoS One* *8*, e56518.
- Miura, K., Matoba, S., Hirose, M., and Ogura, A. (2021). Generation of chimeric mice with spermatozoa fully derived from embryonic stem cells using a triple-target CRISPR method for Nanos3⁺. *Biol. Reprod.* *104*, 223–233.
- Mori, M., Furuhashi, K., Danielsson, J.A., Hirata, Y., Kakiuchi, M., Lin, C.S., Ohta, M., Riccio, P., Takahashi, Y., Xu, X., et al. (2019). Generation of functional lungs via conditional blastocyst complementation using pluripotent stem cells. *Nat. Med.* *25*, 1691–1698.
- Ngo, D., Cheng, Q., O'Connor, A.E., DeBoer, K.D., Lo, C.Y., Beaulieu, E., De Seram, M., Hobbs, R.M., O'Bryan, M.K., and Morand, E.F. (2013). Glucocorticoid-induced leucine zipper (GILZ) regulates testicular FOXO1 activity and spermatogonial stem cell (SSC) function. *PLoS One* *8*, e59149.
- Nishimura, T., Suchy, F.P., Bhadury, J., Igarashi, K.J., Charlesworth, C.T., and Nakauchi, H. (2021). Generation of functional organs using a cell-competitive niche in intra- and inter-species rodent chimeras. *Cell Stem Cell* *28*, 141–149.e3.
- Romero, Y., Vuandaba, M., Suarez, P., Grey, C., Calvel, P., Conne, B., Pearce, D., de Massy, B., Hummler, E., and Nef, S. (2012). The Glucocorticoid-induced leucine zipper (GILZ) is essential for spermatogonial survival and spermatogenesis. *Sex. Dev.* *6*, 169–177.
- Rossant, J., and Frels, W.I. (1980). Interspecific chimeras in mammals: successful production of live chimeras between *Mus musculus* and *Mus caroli*. *Science* *208*, 419–421.
- Saitou, M., and Yamaji, M. (2010). Germ cell specification in mice: signaling, transcription regulation, and epigenetic consequences. *Reproduction* *139*, 931–942.
- Saitou, M., and Miyauchi, H. (2016). Gametogenesis from pluripotent stem cells. *Cell Stem Cell* *18*, 721–735.
- Sambasivan, R., Gayraud-Morel, B., Dumas, G., Cimper, C., Paisant, S., Kelly, R.G., Kelly, R., and Tajbakhsh, S. (2009). Distinct regulatory cascades govern extraocular and pharyngeal arch muscle progenitor cell fates. *Dev. Cell* *16*, 810–821.
- Sommer, C.A., Stadtfeld, M., Murphy, G.J., Hochedlinger, K., Kotton, D.N., and Mostoslavsky, G. (2009). Induced pluripotent stem cell generation using a single lentiviral stem cell cassette. *Stem Cell.* *27*, 543–549.
- Suarez, P.E., Rodriguez, E.G., Soundararajan, R., Mérrillat, A.M., Stehle, J.C., Rotman, S., Roger, T., Voirol, M.J., Wang, J., Gross, O., et al. (2012). The glucocorticoid-induced leucine zipper (gilz/Tsc22d3-2) gene locus plays a crucial role in male fertility. *Mol. Endocrinol.* *26*, 1000–1013.
- Taft, R.A., Low, B.E., Byers, S.L., Murray, S.A., Kutny, P., and Wiles, M.V. (2013). The perfect host: a mouse host embryo facilitating



- more efficient germ line transmission of genetically modified embryonic stem cells. *PLoS One* **8**, e67826.
- Tan, T., Wu, J., Si, C., Dai, S., Zhang, Y., Sun, N., Zhang, E., Shao, H., Si, W., Yang, P., et al. (2021). Chimeric contribution of human extended pluripotent stem cells to monkey embryos ex vivo. *Cell* **184**, 2020–2032.
- Tong, C., Li, P., Wu, N.L., Yan, Y., and Ying, Q.L. (2010). Production of p53 gene knockout rats by homologous recombination in embryonic stem cells. *Nature* **467**, 211–213.
- Tsukiyama, T., Kato-Itoh, M., Nakauchi, H., and Ohinata, Y. (2014). A comprehensive system for generation and evaluation of induced pluripotent stem cells using piggyBac transposition. *PLoS One* **9**, e92973.
- Usui, J.I., Kobayashi, T., Yamaguchi, T., Knisely, A.S., Nishinakamura, R., and Nakauchi, H. (2012). Generation of kidney from pluripotent stem cells via blastocyst complementation. *Am. J. Pathol.* **180**, 2417–2426.
- Wang, X., Shi, H., Zhou, J., Zou, Q., Zhang, Q., Gou, S., Chen, P., Mou, L., Fan, N., Suo, Y., et al. (2020). Generation of rat blood vasculature and hematopoietic cells in rat-mouse chimeras by blastocyst complementation. *J. Genet. Genomics* **47**, 249–261.
- Wu, J., Greely, H.T., Jaenisch, R., Nakauchi, H., Rossant, J., and Belmonte, J.C.I. (2016). Stem cells and interspecies chimeras. *Nature* **540**, 51–59.
- Wu, J., Platero-Luengo, A., Sakurai, M., Sugawara, A., Gil, M.A., Yamauchi, T., Suzuki, K., Bogliotti, Y.S., Cuello, C., Morales Valencia, M., et al. (2017). Interspecies chimerism with mammalian pluripotent stem cells. *Cell* **168**, 473–486.e15.
- Yamaguchi, T., Sato, H., Kato-Itoh, M., Goto, T., Hara, H., Sanbo, M., Mizuno, N., Kobayashi, T., Yanagida, A., Umino, A., et al. (2017). Interspecies organogenesis generates autologous functional islets. *Nature* **542**, 191–196.
- Yamaguchi, T., Sato, H., Kobayashi, T., Kato-Itoh, M., Goto, T., Hara, H., Mizuno, N., Yanagida, A., Umino, A., Hamanaka, S., et al. (2018). An interspecies barrier to tetraploid complementation and chimera formation. *Sci. Rep.* **8**, 15289.
- Yamaji, M., Seki, Y., Kurimoto, K., Yabuta, Y., Yuasa, M., Shigeta, M., Yamanaka, K., Ohinata, Y., and Saitou, M. (2008). Critical function of Prdm14 for the establishment of the germ cell lineage in mice. *Nat. Genet.* **40**, 1016–1022.
- Zhang, H., Huang, J., Li, Z., Qin, G., Zhang, N., Hai, T., Hong, Q., Zheng, Q., Zhang, Y., Song, R., et al. (2018). Rescuing ocular development in an anophthalmic pig by blastocyst complementation. *EMBO Mol. Med.* **10**, e8861.
- Zheng, C., Ballard, E.B., and Wu, J. (2021a). The road to generating transplantable organs: from blastocyst complementation to interspecies chimeras. *Development* **148**, dev195792.
- Zheng, C., Hu, Y., Sakurai, M., Pinzon-Arteaga, C.A., Li, J., Wei, Y., Okamura, D., Ravaux, B., Barlow, H.R., Yu, L., et al. (2021b). Cell competition constitutes a barrier for interspecies chimerism. *Nature* **592**, 272–276.